Acyl-CoA binding protein (ACBP) localizes to ER and Golgi in a ligand dependent manner in mammalian cells

Jesper S Hansen, Nils J Færgeman, Birthe B Kagelund, Jens Knudsen

Acyl-CoA Binding Protein (ACBP) Localizes to ER and Golgi in a Ligand Dependent Manner in Mammalian Cells

Running title:

Intracellular localization and mobility of acyl-CoA binding protein

Jesper S. Hansen*, Nils J. Færgeman*, Birthe B. Kragelund†, Jens Knudsen*, [1]

*Department of Biochemistry and Molecular Biology, University of Southern Denmark, Campusvej 55, DK-5230 Odense M, Denmark, and †Department of Molecular Biology, Ole Maaløes Vej 5, DK-2200 Copenhagen N, Denmark.

[1]To whom correspondence should be addressed (email jkk@bmb.sdu.dk)

Abbreviations used:

Acyl-CoA binding protein, ACBP; BMGE, bovine mammary gland epithelia; bovine serum albumin, BSA; dioleylposphatidylcholine, DOPC; Dulbecco's modified eagle's medium, DMEM; endoplasmic reticulum, ER; fluorescent acyl-CoA indicator, FACI; fatty acid free BSA, FAFBSA; foetal bovine serum, FBS; fluorescence recovery after photobleaching, FRAP; generalized polarization, GP; green fluorescent protein, GFP; hepatocyte nuclear factor-4α, HNF-4α; intensity correlation analysis, ICA; intensity correlation quotient, ICQ; oleic acid, OA; phosphate buffered saline, PBS; Product of the Differences from the Mean, PDM.

SYNOPSIS

In the present study, we microinjected fluorescently labelled liver bovine ACBP (FACI-50), into HeLa and bovine mammary gland epithelial (BMGE) cell lines to characterize the localization and dynamics of ACBP in living cells. Results showed that ACBP targeted to the endoplasmic reticulum (ER) and Golgi in a ligand-binding dependent manner. A variant Y28F/K32A-FACI-50, which is unable to bind acyl-CoA, did no longer show association with ER and became segregated from Golgi, as analysed by intensity correlation calculations. Depletion of fatty acids from cells by addition of fatty acid free BSA (FAFBSA) significantly decreased FACI-50 association with Golgi, while fatty acid overloading increased Golgi-association, strongly supporting that ACBP associates with Golgi in a ligand-dependent manner. Fluorescence recovery after photobleaching (FRAP) showed that the fatty acid induced targeting of FACI-50 to Golgi resulted in a 5-fold reduction in FACI-50 mobility. We suggest that ACBP is targeted to ER and Golgi in a ligand-binding dependent manner in living cells, and propose that ACBP may be involved in vesicular trafficking.

Keywords: ACBP, Golgi, endoplasmic reticulum, trafficking, confocal microscopy, two-photon excitation FRAP.

INTRODUCTION

ACBP is a highly conserved protein from protozoa to humans [1], which suggests that the protein is required for very basic functions conserved throughout the eukaryotic kingdom. Our understanding of the function of ACBP is still incomplete. *In vitro* studies have shown that ACBP desorbs acyl-CoA esters embedded in immobilised synthetic lipid membranes and donates acyl-CoA to β-oxidation in mitochondria or glyerolipid synthesis in microsomes [2, 3], suggesting that ACBP acts as an acyl-CoA transporter. Depletion of ACBP (Acb1p) from yeast *S. cerivisiae* results in strongly reduced growth, accumulation of large amounts of cytoplasmic vesicles and multi layered plasma membranes and fragmented vacuoles [4]. The vacuoles isolated from the Acb1p depleted strain lack important SNARE proteins and are unable to undergo homeotypic fusion [4]. This indicates that ACBP in yeast may play a role in vesicular trafficking. The Acb1p depleted strain also shows strongly reduced ceramide levels [5], indicating also a role for ACBP in long chain base synthesis and/or fatty acid

elongation. The finding that a *C. elegans* ACBP domain protein MAA-1 is required for vesicular transport between the plasma membrane and Golgi complex [6] further suggests a role of the ACBP domain in vesicular trafficking. Experimental evidence also suggest that ACBP plays a role in the regulation of hepatocyte nuclear factor-4α (HNF-4α) [7] and further interacts with the $GABA_{A\alpha1}$ subunit in rabbit Müller cells [8]. Finally, ACBP has been shown to augment Bid induced mitochondrial damage and cell death by activating μ-calpain. [9].

Knowledge of the intracellular localization and movement of ACBP in living cells would be of great value in assigning a function in specific processes. Numerous *in vitro* studies have been carried out to characterize the cellular localization of the basal 82 – 92 residue ACBP (see ref. [10] for review). Subcellular fractionation and immunohistochemical studies at the level of electron microscopy report that ACBP can be found in the cytosol associated with smooth endoplasmic reticulum, Golgi, outer membrane of mitochondria and around large cytoplasmic vesicles [11-20]. Studies with the horn worm *M. secta* intestinal columnar cells and prothoracic gland ecdystereogenic cells [19] and 3T3-L1 cells [21] show that ACBP in addition of being present in the cytosol also appears in the nucleus.

The existing experimental results draw a very confused picture of the possible intracellular localization of ACBP and do not add to our understanding of the biological function of the protein. A further complication in the interpretation of the immunohistochemical and immunofluorescence data is that ACBP can not be fixed by conventional protein denaturizing methods. After denaturation with TCA, ACBP readily re-dissolve in buffered solutions at neutral pH (our unpublished results). Hence, incomplete fixing of ACBP will result in loss of ACBP during the immunostaining process.

To circumvent the above mentioned problems we have in the present work visualized the cellular localisation of ACBP in living HeLa and the bovine mammary gland epithelial (BMGE) cells using microinjection of fluorescently labelled bovine L-ACBP (FACI-50, [22]). The results show that ACBP localizes to the endoplasmic reticulum and Golgi complex in a ligand dependent manner.

EXPERIMENTAL

Reagents

Nuclon angle necked T_{75} culture flasks with filter caps were from NUNC A/S (Roskilde, Denmark). Uncoated 50 mm glass-bottom culture dishes were from MatTek

Corporation (Ashland, MA, USA). Dulbecco's modified eagle's medium (DMEM) and Prolactin (Luteotropic hormone, LTH) were purchased from Sigma-Aldrich Denmark A/S (Brøndby, Denmark). Foetal bovine serum, MEM non-essential amino acids (100×) solution, Penicillin-Streptomycin (10,000 units of penicillin (base) and 10,000 µg of streptomycin (base)/ml)) and L-glutamine 200 mM (100×) liquid were from Invitrogen A/S (Taastrup, Denmark). Actrapid-Insulin was from Novo Nordisk A/S (Bagsværd, Denmark). Hydrocortisone was from SERVA Electrophoresis (Heidelberg, Germany). Sterile Femtotips for microinjection and Femtotip microloaders (2-20 µl) were from Eppendorf AG (Hamburg, Germany). The organelle specific fluorescent markers glibenclamide-BODIPY TR, MitoTracker Red CM-H_2XRos, LysoTracker Red DND-99, BODIPY493/503 neutral lipid stain and BOPIPY TR C_5-ceramide complexed to BSA were from Molecular Probes Inc. (Eugene, OR, USA). 6-Bromoacetyl-2-dimethylaminonapthalene (badan) was from AnaSpec (San Jose, CA, USA).

Site-directed mutagenesis, protein expression, purification and badan labelling

Protein expression, purification and badan labelling of Lys50Cys-ACBP and of Met24Cys-ACBP to produce FACI-50 and FACI-24, respectively, were carried out as previously described [23].

A variant of FACI-50 was constructed by introducing two additional amino acid substitutions; Tyr28Phe and Lys32Ala, into the existing Lys50Cys-ACBP plasmid. Site-directed mutagenesis was carried out as previously described [24]. The primers used for amplification of mutant bovine ACBP were 5´-GTAGTGAGAGAAGATGAACAACATTTC-3' upstream (Tyr28Phe) and 5´-GCTCAAGCTACCGTTGGTGACATCAAC-3' downstream (Lys32Ala). Underlined bases indicate substitutions. Protein expression, purification and badan labelling of bovine Tyr28Phe, Lys32Ala, Lys50Cys-ACBP to produce Y28F/K32A-FACI-50 was carried as for FACI-50 [23].

Ligand binding studies of FACI-24, FACI-50 and Y28F/K32A-FACI-50

Dissociation constants of FACI-24, FACI-50 and Y28F/K32A-FACI-50 were determined by isothermal microcalorimetry essentially as described previously [25], except that the buffer used was 20 mM MES, 100 mM NaCl, pH 6.8.

Cell culture

HeLa cells were cultured in T_{75}-culture flasks in Dulbecco's modified eagle's medium (DMEM) added penicillin (50 U/ml), streptomycin (50 μg/ml) ($DMEM_{pen/strep}$), 10% (v/v) foetal bovine serum (FBS), 0.1 mM non-essential amino acids and 10 mM L-glutamine, in a humidified incubator at 37°C in the presence of 5% CO_2. Media was exchanged every 2 days and the cells subcultured at preconfluent densities using 0.25% (w/v) trypsin and 0.03% (w/v) EDTA in phosphate buffered saline (PBS), pH 7.4 (trypsin/EDTA solution).

The bovine mammary gland epithelial cells (BMGE) originated from [26], and were kindly provided by Professor Karsten Kristiansen, University of Southern Denmark, Denmark. BMGE cells were cultured in T_{75}-culture flasks in $DMEM_{pen/strep}$ supplemented with 20% (v/v) FBS, 10 mM L-glutamine and insulin, hydrocortisone, and prolactin (1.0 μg/ml each) in a humidified incubator at 37°C in the presence of 5% CO_2 [26-28]. Cells were subcultured at pre-confluent densities using trypsin/EDTA solution as described above.

Establishment of stable HeLa cell lines expressing GFP or GFP-ACBP

The expression vectors pEGFP-C1 with and without bovine liver ACBP inserted, respectively, were obtained from Professor Karsten Kristiansen, University of Southern Denmark. The day before transfection, HeLa cells ($2\text{-}6\times10^6$ cells) were plated into 60 mm culture petri dishes containing 4 ml DMEM supplemented with 10% FBS and without antibiotics. HeLa cells were transfected with ACBP-GFP vector or empty vector using LipofectAMINE PLUS Reagent (Gibco Life Technologies, Rockville, Maryland, USA). The transfection procedure was based on the manufactures' protocol and adapted to 60-mm petri dishes.

The transfected cell populations were maintained in complete DMEM supplemented with 0.5 mg/ml G418, and cells were split at a ratio of 1:10 twice a week. Cells transfected

with expression vector alone served as controls. For imaging experiments, cells were grown on glass-bottom Petri dishes (MatTek Corporation, Ashland, MA, USA).

Microinjection of HeLa and BMGE cells

For microinjection experiments, cells that had been grown to sub-confluence were dissociated from the plates by treatment with trypsin/EDTA solution for 5 min. at 37°C. An aliquot of 1 x 10^5 cells was plated on 50-mm diameter glass-bottom culture dishes (MatTek Corporation, Ashland, MA, USA) and cultured to 70-80% confluence in culture medium. Immediately before microinjection, the medium was removed and replaced by C-HEPES buffer pre-equilibrated to 37°C. Microinjection was performed at room temperature using a microinjection system consisting of an Eppendorf Microinjector 5242 and a Micromanipulator 5170 (Eppendorf, Netherlands) attached to the side of a Leica DMIRBE inverted microscope (Leica Micosystems, Wetzlar, GmbH). Microinjection was performed using a 40× objective. HeLa and BMGE cells were microinjected with 200 µM and 400 µM, respectively, of FACI-50 or Y28F/K32A-FACI-50 dissolved in PBS, pH 7.4. The FACI solutions were centrifuged (14,000 rpm, 4°C, 10 m) immediately before use. Sterile Femtotips (Eppendorf) were back-filled with 2 µl of the FACI solutions using Microloader tips (Eppendorf) and placed with a 45° angle over the Petri dish. Injection was executed with the automatic inject function of the system, while injection time was set to 0.5 s. The compensation pressure was set to 25 hPa and injection pressure was adjusted to 100 hPa for HeLa cells and 130 hPa for BMGE cells, respectively.

Double labelling experiments by confocal and two-photon laser excitation microscopy

Microscopy was performed on a confocal microscope (model LSM 510 META; Carl Zeiss MicroImaging Inc., Jena, Germany) using a 40x/1.2 numerical aperature (NA) Plan-Apochromat water-immersion lens, unless otherwise stated. Acquisition was performed using LSM 510 version 3.0 software (Carl Zeiss MicroImaging Inc., Jena, Germany).

For transfected cells, GFP fluorescence was excited at 488 nm with a 30-mW Argon/2 laser and images were collected using a primary HFT 488 dichroic beam splitter and a 505 nm long pass filter. The nucleus of GFP-transfected cells were identified by incubating cells for 60 min with 16 µM of DAPI dissolved in C-HEPES buffer.

For FACI experiments, the 50-mm glass-bottom culture dishes were immediately after microinjection transferred to a heated (37.5°C) microscope stage (TempControl Digital 37–2

device; Warner Instruments) with a custom made aluminium insert to fit the 50-mm glass-bottom culture dishes. FACI injected cells were identified by shortly switching on/off a blue reflector by which FACI positive cells exhibited a bright green appearance.

For image acquisition, blue fluorophores (DAPI and FACIs) were excited using two-photon excitation laser scanning microscopy. Excitation was provided by a tuneable, broadband, mode-locked titanium:sapphire Mai Tai laser (Spectra-Physics Lasers, California, USA) at 800 nm, which was reflected by a primary HFT KP 650 dichroic mirror, fluorescence filtered with a secondary NFT 490 dichroic mirror and emission recorded with a 435-485 nm band pass filter.

The endoplasmic reticulum was labelled by incubating cells with 2 μM of glibenclamide-BODIPY TR in C-HEPES buffer at 37°C in 5% CO_2 for 30 min.

Golgi complex was identified with BOPIPY TR C_5-ceramide (Molecular Probes) as follows: cells were incubated with 5 μM BODIPY TR C_5-ceramide complexed to BSA in C-HEPES buffer for 30 min at 37°C. Cells were then washed with C-HEPES buffer and incubated in $DMEM_{pen/strep}$ with serum for further 30 min at 37°C.

Mitochondria were visualized using MitoTracker Red CM-H_2XRos with a final concentration of 0.5 μM in $DMEM_{pen/strep}$ culture medium without serum. Cells were labelled for 45 min at 37°C in 5% CO_2.

Labelling of lysosomal vesicles was performed by incubating cells with 75 nM of Lysotracker Red DND-99 in $DMEM_{pen/strep}$ without serum at 37°C in 5% CO_2 for 30 min.

Image acquisitions of Glibenclamide-BODIPY TR, BODIPY TR C_5-ceramide, MitoTracker Red CM-H_2XRos and Lysotracker Red DND-99 were performed with excitation at 543 nm provided by a 1-mV Helium/Neon1 (HeNe/1) laser, and emission collected using a primary HFT488/543/633 dichroic beam splitter, a secondary NFT 545 dichroic mirror and a 565-615 nm band pass filter.

Lipid droplets and endogenous membranes were identified using BODIPY493/503 BODIPY493/503 neutral lipid stain. Labelling were performed by incubating cells with 10 μg/ml of this lipophilic dye dissolved in C-HEPES at 37°C in 5% CO_2 for 45 min. For imaging, BODIPY493/503 was excited at 488 nm using a 30-mV Argon/2 laser and emission collected using a primary HFT 488 dichroic beam splitter and a 500-530 IR band pass filter.

For double labelling experiments, the two channels were scanned alternately in a line-by-line fashion, having only one laser line and one detector channel on at each time. Acquisition of confocal fluorescence images was performed using a pinhole diameter corresponding to 1 Airy unit unless otherwise stated. Images were assessed using the LSM Browser (Carl Zeiss MicroImaging, Inc.) and processed using ImageJ open-source software (http://rsb.info.nih.gov/ij).

Quantitative co-localization analysis

Co-localization of FACI-50 or Y28F/K32A-FACI-50, respectively, with organelle specific dyes was performed using the intensity correlation analysis (ICA) method described by Li *et al.*, 2004 [29]. The ICA method tests for co-localization by comparing how the intensity of two signals varies with respect to each other, i.e. it tests their synchrony. With random staining, the intensity correlation quotient (ICQ) = ~0; dependent staining $0 < ICQ \leq +0.5$, whereas for segregated staining $0 > ICQ \geq -0.5$ [29]. Pre-existing defined immunofluorescence images of random, dependent and segregated staining, respectively, were used as controls.

Product of the Differences from the Mean (PDM), i.e. for each pixel is defined as (channel 1 intensity – mean channel 1 intensity)×(channel 2 intensity – mean channel 2 intensity), which is equal to the (A–a)×(B–b) described by Li *et al.*, 2004 [29]. ICA plots represent the fluorescence intensities of one channel as a function of the respective PDM values of both recording channels.

The software for quantitative co-localization analysis was provided as a plug-in (written by Elise Stanley, Toronto, Canada) to ImageJ.

FACI-50 generalized polarization (GP) measurements

The fluorescence emission properties of FACI-50 are sensitive to the polarity of the local environment of the fluorescent probe badan. Saturating amounts of CoA shift the maximum emission yield of FACI-50 from 510 nm to 490 nm, acyl-CoA binding in contrast causes a red-shift of FACI-50 emission [22]. Emission spectral changes can be quantified comparing generalized polarization (GP) values for shifted and un-shifted fluorescence intensity peaks of FACI-50. GP values were calculated by: $GP = I_b\text{-}I_g/I_b+I_g$, where I_b and I_g

correspond to the intensities at the blue and green edges of the emission spectrum, respectively [30, 31]. *In vitro* fluorescence spectra were measured using a Chronos ISS fluorimeter (ISS, Champaign, IL, USA) with excitation wavelength at 374 nm using a laser diode as excitation source. I_b and I_g were measured at 470 nm and 520 nm respectively. Two-photon excitation (800 nm) GP images of FACI-50 microinjected BMGE cells in C-HEPES buffer covering 435-465 nm and 535-565 nm range, respectively were obtained simultaneously in dual-channel setup on a confocal microscope (model LSM 510 META; Carl Zeiss MicroImaging Inc., Jena, Germany). The objective used was a 40x/1.2 NA Plan-Apochromat water-immersion. The two images were analyzed using SimFCS software (Laboratory for Fluorescence Dynamics, IL, USA) to obtain the GP image and the associated GP histogram (distribution of the GP values per pixel).

Effect of defatted BSA and fatty acid addition on ACBP localization

FACI-50 microinjected BMGE cells pre-labelled with BOPIPY TR C_5-ceramide as described above were incubated for 10 min in C-HEPES buffer containing 600 µM FAFBSA or BSA complexed with 2.66 mM oleic acid (OA/BSA) to give a OA/BSA molar ratio of 4.44, resulting in a free oleic acid concentration [FFA_{OA}] of 150 nM as described previously [32, 33]. The OA/BSA complexes were made by mixing stock solutions of 1.0 mM FAFBSA solution in C-HEPES with 50 mM oleic acid sodium salts dissolved in C-HEPES to give a final BSA and oleic acid concentration of 600 µM and 2.66 mM, respectively (OA/BSA ratio of 4.44) [33].

Two-photon excitation FRAP experiments

To measure the mobility of FACI-50 in the Golgi complex of BMGE cells treated with FAFBSA or the OA/BSA complexes for 30 minutes, FRAP experiments were performed essentially as described [34]. Fluorescence recovery curves were fitted using SIGMAPLOT scientific graphing software (San Rafael, CA, USA) and half time recoveries were calculated as described [35].

Circular Dichroism (CD) spectroscopy

Far-UV CD spectra of r-bovine L-ACBP, FACI-50, FACI-24 and Y28F/K32A-FACI-50 were recorded on a Jasco J-810 spectro-polarimeter scanning wavelengths in the range

250-190 nm, averaging over 4-6 scans per experiment, data pitch of 0.1 nm and scan rate 20 nm/min at room temperature. Total protein concentration was 10 μM and the proteins were diluted from stocks into either Milli Q water or 10 mM NaH_2PO_4, pH 7.4. The cuvettes used were 0.1 cm Quartz-Suprasil from Hellma. Reference spectra of buffer or water were recorded during each session and subtracted accordingly. Each sample was allowed at least 10 min to reach equilibrium before spectrum acquisition.

RESULTS

A GFP-ACBP fusion protein expressed in HepG2 cells was found to localise to both the cytoplasm and to the nucleus [21]. However, no GFP expression control was reported in these experiments. We explored the possibility of using stable expression of GFP-ACBP to map the intracellular localisation of ACBP in HeLa cells. The results showed that localization of the GFP-ACBP can not be distinguished from that of GFP on its own (Figure 1). This shows that the GFP-ACBP fusion is unsuitable for studying the intracellular localization of basal 82-92 residue ACBP *in vivo*. There might be several reasons for this. First, GFP in it self is ~3.0 times larger than the ACBP and might therefore physically hinder interaction of the ACBP-GFP fusion protein with potential ACBP interaction partners. Secondly, GFP on its own has been show to target to organelles including the nucleus [36]. This could, if GFP is the dominating part of the fusion protein, provide misleading results.

ACBP localizes to the endoplasmic reticulum and Golgi complex in HeLa cells

Fluorescence emission of FACI-50 injected HeLa cells shows that bovine FACI-50 is highly concentrated close to the nucleus with moderate fluorescence intensity of the perinuclear membrane typical for the localization to Golgi and endoplasmic reticulum (ER) (results not shown). The nucleus itself and the remaining cytosol show much lower fluorescence emission intensities. Co-staining of FACI-50 microinjected HeLa cells with glibenclamide-BODIPY or the structural Golgi marker BODIPY TR C_5-ceramide strongly indicate co-localization of ACBP to both the ER and to Golgi with an intensity correlation quotient (ICQ) of 0.193 and 0.135 respectively.

Although, the sequences of bovine and human L-ACBP show 94% identity it could be argued that the use of a bovine L-ACBP based probe in the human derived HeLa cell line is

non-physiological. We therefore switched to bovine mammary gland epithelial cell line (BMGE).

Localization of ACBP to the ER and Golgi complex of BMGE cells is ligand dependent

In contrast to HeLa cells, BMGE cells represent a much more homogenously shaped cell population. BMGE cells are morphologically large, very flat cells and in the light microscope the nucleus and surrounding membranous organelles can be clearly distinguished from the remaining cytosol. This makes delivery of FACI-50 into the cytosol by microinjection easier compared to HeLa cells, and thus significantly reduces the risk of injection the fluorescent probe into or near the nucleus, which could lead to incorrect interpretation of ACBP localization results.

Microinjection of FACI-50 into BMGE cells confirms that ACBP localizes to ER and Golgi as seen in HeLa cells (Figure 2A and 3A). In contrast, we were unable to show co-localization of FACI-50 with mitochondria, lysosomes or fat droplets when microinjection of FACI-50 into BMGE cells incubated with MitoTracker Red CM-H_2XRos, LysoTracker Red DND-99 or the neutral lipid stain BODIPY493/503, respectively, were performed (Suplementery data, Figure 1, 2 and 3). In order to test the importance of ligand binding for association of ACBP with ER/Golgi we produced by site-directed mutagenesis a FACI-50 variant with impaired ligand binding ability, Y28F/K32A-FACI-50. The Y28F/K32A site-directed mutations in yeast ACBP have previously been shown to reduce dodecanoyl-CoA binding of native bovine ACBP with about 1000 fold (our unpublished result).

Isothermal titration microcalorimetry of FACI-24, FACI-50 and Y28F/K32A-FACI-50, respectively, determined the dissociation constant (K_d) of myristoyl-CoA binding to FACI-24 and FACI-50 to 62 ± 25 nM (n=2) and 177 ± 52 nM (n = 3), respectively. However Y28F/K32A-FACI-50 could not be shown to bind myristoyl-CoA at all (results not shown). Fold integrity of all three FACI-variants was confirmed from far-UV CD spectral analysis (Supplementary data, Figure 4) demonstrating that the effect from mutations and fluorescence labelling were directly on ligand binding, and clearly not on structure The disruption of ligand binding activity strongly perturbed the intracellular localization of ACBP, resulting in an even distribution of Y28F/K32A-FACI-50 throughout the whole cell including the nucleus (Figure 2B and 3B). The ICQ for co-localization between ER-staining and FACI-50 and Y28F/K32A-FACI-50 staining were 0.30 and 0.038, respectively, and between Golgi and FACI-50 and

Y28F/K32A-FACI-50 staining 0.28 and -0.15 respectively. The low (0.038) or negative (-0.15) ICQs for co-staining of Y28F/K32A-FACI-50 with ER or with Golgi alone, respectively, show that association of the mutant protein with ER is random and that it is segregated from Golgi. This suggests that ligand binding target ACBP to ER/Golgi.

If this hypothesis holds it should be possible to obtain similar changes in FACI-50 intracellular localization by manipulating the intracellular concentration of acyl-CoA levels. The intracellular concentration of free fatty acids and acyl-CoA is strongly affected by the concentration of free fatty acids in the media [32, 37]. We therefore performed ICA measurements on FACI-50 co-localisation with ER and Golgi in cells pre-incubated with either FAFBSA or OA/BSA (4.44, molar ratio) in order to deplete or overload, respectively the cells with fatty acids. Addition of FAFBSA to the medium caused a reduction in the ICA coefficient for FACI-50 co-localization/association with the Golgi marker from 0.128 ± 0.011 to 0.088 ± 0.009. On the contrary, addition of OA/BSA acid resulted in an increased ICA coefficient for FACI-50 association with Golgi from 0.088 ± 0.009 to 0.190 ± 0.013 (Figure 4). This observation further supports the notion that ligand binding is essential for targeting of ACBP to Golgi. It should be noted that the apparent overall lower ICQ of co-staining BMGE cells with FACI-50 and BOPIPY TR C_5-ceramide in the BSA and OA/BSA challenging experiments was due to an 8-fold increase in image acquisition scan times, which reduces photobleaching of the fluorophores but also lowers the image resolution.

To exclude the possibility that the ligand dependent FACI-50/Golgi interaction could be caused by the presence of badan on the surface of FACI-50 in the ligand bound state the experiments reported in figure 4 were repeated with FACI-24 in which the fluorophore is buried underneath acyl-CoA in the holo-ACBP complex. FACI-24 exhibited the same ligand dependent interaction with Golgi as FACI-50 (results not shown), excluding that the FACI-50/acyl-CoA interaction with Golgi is caused by the badan side chain.

Generalized polarization measurements of FACI-50 *in vivo*

Bovine L-ACBP binds free CoA with about 1000 fold lower affinity (K_d ~2 μM, [38]) than it binds palmitoyl-CoA (2-8 nM, [39]). Binding of CoA to FACI-50 causes a downshift in fluorescence emission maximum from 510 nm to 490 nm (figure 5 and [22]). However, FACI-50 and FACI-50/oleyl-CoA emission spectra could not be differentiated. The calculated

GP values for the apo-FACI-50, FACI-50/oleyl-CoA and FACI-50/CoA *in vitro* spectre recorded in figure 5 were -0.361 ± 0.001, -0.375 ± 0.004 and -0.004 ± 0.002 respectively. Therefore, GP measurements can be used to distinguish between FACI-50/CoA and apo-FACI-50 plus acyl-CoA/FACI 50. The determined *in vivo* GP value of -0.401 (Figure 5) were in the same range as *in vitro* GP values of apo-FACI-50 (-0.361) and oleyl-CoA/FACI-50 (-0.375), respectively and significantly different from the *in vitro* FACI-50/CoA GP value This strongly suggest that that ACBP *in vivo* is present as either apo-ACBP or acyl-CoA/ACBP and not in complexes with CoA.

ACBP mobility in Golgi is highly affected by endogenous fatty acid levels

The fact that addition of OA/BSA to the incubation medium results in increased co-localisation with Golgi (Figure 4) combined with the fact that disruption of ligand binding capability segregates FACI-50 from Golgi confirms the hypothesis that ligand binding is essential and targets ACBP to Golgi. This notion is further supported by FRAP analysis, which showed that the fluorescence recovery half time of FACI-50 in the Golgi complex of BMGE cells increased from 0.8 ± 0.4 s in C-HEPES buffer to 3.7 ± 0.6 s in C-HEPES plus OA/BSA in the culture medium (Figure 6). FRAP experiments on FACI-50 injected BMGE cells incubated with FAFBSA did not alter ACBP mobility compared to cells incubated in C-HEPES buffer alone (data not shown). A 5-fold reduction in FACI-50 mobility in the presence of OA/BSA in the culture medium strongly suggests that acyl-CoA binding targets FACI-50 to Golgi and that FACI-50 actually transient associated with Golgi.

DISCUSSION

Previous experimental data of the intracellular distribution of ACBP using indirect immunofluorescence or immunogold electron microscopy have, as pointed out in the introduction, yielded variable results from ACBP being exclusively cytosolic in Leydig cells [11-13] or found in the nucleus only of undifferentiated 3T3-L1 pre-adipocytes or in both the nucleus and cytosol of differentiated 3T3-L1 cells [21]. In other cells, including rat testes Leydig, Sertoli and seminiferous tubule cells, ACBP distributed over the whole cytosol, but was also found at the smooth endoplasmic reticulum, Golgi and outer membrane of mitochondria [12]. In some cells such as rat Stilling's cells, ACBP was concentrated around

large cytoplasmic vesicles [17]. The value of these previous experimental data may be questioned also due to the technical problems mentioned above.

In the present work we circumvented these difficulties by performing live-cell imaging on microinjected fluorescently labelled ACBP in Hela and BMGE cells. The results show that although ACBP was found throughout the whole cell including in the nucleus, it distributes in a very heterogeneous manner. ACBP was found to be highly enriched on the ER, Golgi and the perinuclear membrane with lower concentrations seen in the cytosol and in the nucleus. A finding that is in agreement with what has previously been found by indirect immunohistochemistry in rat hepathoma cells [7] and L-cell fibroblasts. [20]. The co-localization of FACI-50 with both ER and Golgi was confirmed by co-staining FACI-50 injected cells with organelle specific stains of these two compartments and calculating the intensity correlation quotient (ICQ) between the FACI-50 and organelle dye emission fluorescence. The calculated ICQs for FACI-50 co-localization with ER and Golgi stains in BMGE cells suggest strong interaction with both compartments. The Y28F/K32A-FACI-50 mutations which disrupt myriostyl-CoA binding, but retain overall three-dimensional structure of the protein, reduced the ICQ for co-localization between ER and Golgi staining from 0.30 and 0.28 for FACI-50, respectively to 0.038 and -0.15 for Y28F/K32A-FACI-50 staining, respectively, showing that Y28F/K32A-FACI-50 no longer associates with ER and segregates from Golgi. It has previously been shown that the intracellular concentration of free fatty acids and acyl-CoA is strongly affected by the concentration of free fatty acids in the media [32, 37]. The present work shows that ACBP is likely to occur as apo-ACBP or ACBP/acyl-CoA, and not as ACBP/CoA complex *in vivo*. Increasing the cellular concentration of acyl-CoA would therefore be expected to increase the concentration of ACBP/acyl-CoA. If ligand binding is required to target ACBP to ER and Golgi, it should be possible to alter ACBP association with the two organelles by manipulating the fatty concentration in the culture media. Our results show that this is indeed the case. Addition of FAFBSA to the BMGE cell culture media, which will extract fatty acids from the cells, reduced the ICQ for FACI-50 association with Golgi, from 0.12 to ~0.09 whereas addition of OA/BSA increased the ICQ to ~0.18 (Figure 4). The fact that addition of OA/BSA to the media, in addition to increase the ICQ, also reduced the mobility of FACI-50 associated with Golgi by 5-fold as shown by FRAP experiments (Figure 6) strongly supports the perception that ligand binding targets ACBP to the Golgi.

The functional association of ACBP with both ER and Golgi opens new windows for interpretations of ACBP function in relation to the existing published literature data. Long chain acyl-CoA synthetase activity is predominantly found on microsomes (73%) mitochondria (20%) and in peroxisomes (7%) [40] but not on Golgi. Targeting of ACBP to ER in a ligand dependent manner would therefore make sense since the majority of acyl-CoA synthases and lipid synthesizing acyl-transferases are found on the ER. In this respect it is interesting that ACBP has been shown to co-localize with acyl CoA:cholesterol acyltransferase (ACAT) in the ER and perinuclear region in L-cell fibroblasts [20]. Golgi has not been reported to contain acyl-CoA synthetase activity, but it has been reported to harbour lysophospholipid acyltransferases that have been suggested to co-ordinately regulate Golgi membrane shape and tubule formation [41] as well as protein acylation [42]. These observations provide a possible explanation for the long known requirement of acyl-CoA for vesicle fusion and budding [43-46]. The present result showing that ACBP gets targeted to Golgi in a ligand dependent manner makes acyl-CoA/ACBP a likely candidate for donating acyl-CoA esters required for budding and fusion. Previous data show that Acb1p (ACBP) depleted yeast show all signs of perturbed vesicle trafficking including: 1) accumulation of numerous small vesicles in the cytosol, 2) appearance of fragmented vacuoles unable to fuse do to the lack of essential snare proteins, 3) appearance of multi layered plasma membrane and 4) induction of increased uptake of the accumulating vesicles in the vacuole by micro autophagocytosis [4]. The observation that the *C. elegans* MAA-1 ACBP domain protein participates in plasma membrane endosomal vesicle recycling confirms a role of ACBP proteins in donating acyl-CoA required for fusion and budding of vesicles [6].

ACBP does not contain any specific organelle targeting sequences, except for a potential endoplasmic reticulum retrieval signal consisting of a di-lysine (KK) motif near the C-terminus [47]. However, this sequence motif is only conserved in a limited number of mammalian basal ACBP isoforms [48]. The present results show this sequence motif in it self is unable to target bovine L-ACBP to ER and Golgi and that ligand binding is essential and required to target FACI-50 to Golgi. The actual mechanism by which ACBP attach to the membrane is presently unknown. It has been reported that ACBP interacts with charged lipids in a membrane curvature dependent manner [49]. However, these experiments were carried out at very low ionic strength and can not be repeated at physiological ionic strength using isothermal titration calorimetry (our unpublished results). Recent results obtained by atomic

force microscopy have shown that bovine L-ACBP/palmitoyl-CoA associate with dioleylposphatidylcholine (DOPC) linear membranes [3]. A possible mechanistic explanation for this association could be an exchange of the palmitoyl-acyl chain of the ACBP bound acyl-CoA with an oleyl-acyl chain from a DOPC molecule in the membrane. This would leave the CoA head group bound in the binding site, with the palmitoyl-chain immersed in the DOPC bilayer, stabilized by the PC-oleyl chain flipping out from the membrane and into the ACBP/acyl-CoA binding site. The observation that two human L-ACBP molecules have the ability to share one intact dodecanoyl-CoA molecule having the head group bound in the one ACBP and the acyl-chain in the other ACBP binding site stabilised by a free fatty acid bound in one ACBP and a 4-phosphopanteteine fragment in the other ACBP [50] supports the above suggested model for ACBP/acyl-CoA membrane binding. Alternatively, ACBP could interact with proteins residing in either the ER and/or the Golgi apparatus, which is currently being investigated.

ACKNOWLEDGEMENT

This work was supported by a grant to Jens Knudsen from The Danish Natural Science Research Council. The authors want to thank Dr. Louis Bagatolli and Dr. Daniel Wüstner University of Southern Denmark for advice and technical assistance concerning fluorescence microscopy.

REFERENCES

1 Burton, M., Rose, T. M., Faergeman, N. J. and Knudsen, J. (2005) Evolution of the acyl-CoA binding protein (ACBP). Biochem J **392**, 299-307

2 Rasmussen, J. T., Faergeman, N. J., Kristiansen, K. and Knudsen, J. (1994) Acyl-CoA-binding protein (ACBP) can mediate intermembrane acyl-CoA transport and donate acyl-CoA for beta-oxidation and glycerolipid synthesis. Biochem. J. **299 (Pt 1)**, 165-70

3 Cohen Simonsen, A., Bernchou Jensen, U., Faergeman, N. J., Knudsen, J. and Mouritsen, O. G. (2003) Acyl-coenzyme A organizes laterally in membranes and is recognized specifically by acyl-coenzyme A binding protein. FEBS Lett. **552**, 253-8

4 Faergeman, N. J., Feddersen, S., Christiansen, J. K., Larsen, M. K., Schneiter, R., Ungermann, C., Mutenda, K., Roepstorff, P. and Knudsen, J. (2004) Acyl-CoA-

binding protein, Acb1p, is required for normal vacuole function and ceramide synthesis in Saccharomyces cerevisiae. Biochem. J. **380**, 907-18

5 Gaigg, B., Neergaard, T. B., Schneiter, R., Hansen, J. K., Faergeman, N. J., Jensen, N. A., Andersen, J. R., Friis, J., Sandhoff, R., Schroder, H. D. and Knudsen, J. (2001) Depletion of acyl-coenzyme A-binding protein affects sphingolipid synthesis and causes vesicle accumulation and membrane defects in Saccharomyces cerevisiae. Mol. Biol. Cell **12**, 1147-60

6 Larsen, M. K., Tuck, S., Faergeman, N. J. and Knudsen, J. (2006) MAA-1, a Novel Acyl-CoA-binding Protein Involved in Endosomal Vesicle Transport in Caenorhabditis elegans. Mol. Biol. Cell

7 Petrescu, A. D., Payne, H. R., Boedecker, A., Chao, H., Hertz, R., Bar-Tana, J., Schroeder, F. and Kier, A. B. (2003) Physical and functional interaction of Acyl-CoA-binding protein with hepatocyte nuclear factor-4 alpha. J. Biol. Chem. **278**, 51813-24

8 Barmack, N. H., Bilderback, T. R., Liu, H., Qian, Z. and Yakhnitsa, V. (2004) Activity-dependent expression of acyl-coenzyme a-binding protein in retinal muller glial cells evoked by optokinetic stimulation. J. Neurosci. **24**, 1023-33

9 Shulga, N. and Pastorino, J. G. (2006) Acyl coenzyme a binding protein augments bid induced mitochondrial damage and cell death by activating mu - calpain. J. Biol. Chem.

10 Knudsen, J., Burton, M. and Færgeman, N. (2004) Long chain acyl-CoA esters and acyl-CoA binding protein (ACBP) in cell function. Advances in Molecular and Cell Biology **33**, 123-153

11 Rheaume, E., Tonon, M. C., Smih, F., Simard, J., Desy, L., Vaudry, H. and Pelletier, G. (1990) Localization of the endogenous benzodiazepine ligand octadecaneuropeptide in the rat testis. Endocrinology **127**, 1986-94

12 Schultz, R., Pelto-Huikko, M. and Alho, H. (1992) Expression of diazepam binding inhibitor-like immunoreactivity in rat testis is dependent on pituitary hormones. Endocrinology **130**, 3200-6

13 Duparc, C., Lefebvre, H., Tonon, M. C., Vaudry, H. and Kuhn, J. M. (2003) Characterization of endozepines in the human testicular tissue: effect of triakontatetraneuropeptide on testosterone secretion. J. Clin. Endocrinol. Metab. **88**, 5521-8

17

14 Knudsen, J., Hojrup, P., Hansen, H. O., Hansen, H. F. and Roepstorff, P. (1989) Acyl-CoA-binding protein in the rat. Purification, binding characteristics, tissue concentrations and amino acid sequence. Biochem. J. **262**, 513-9

15 Alho, H., Varga, V. and Krueger, K. E. (1994) Expression of mitochondrial benzodiazepine receptor and its putative endogenous ligand diazepam binding inhibitor in cultured primary astrocytes and C-6 cells: relation to cell growth. Cell Growth Differ. **5**, 1005-14

16 Johansson, O., Hilliges, M., Ostenson, C. G., Sandberg, E., Efendic, S. and Mutt, V. (1991) Immunohistochemical localization of porcine diazepam-binding inhibitor (DBI) to rat endocrine pancreas. Cell Tissue Res. **263**, 395-8

17 Lesouhaitier, O., Feuilloley, M., Lihrmann, I., Ugo, I., Fasolo, A., Tonon, M. C. and Vaudry, H. (1996) Localization of diazepam-binding inhibitor-related peptides and peripheral type benzodiazepine receptors in the frog adrenal gland. Cell. Tissue Res. **283**, 403-12

18 Toranzo, D., Tong, Y., Tonon, M. C., Vaudry, H. and Pelletier, G. (1994) Localization of diazepam-binding inhibitor and peripheral type benzodiazepine binding sites in the rat ovary. Anat. Embryol. (Berl.) **190**, 383-8

19 Snyder, M. J. and Antwerpen, R. V. (1997) Cellular distribution, levels, and function of the diazepam-binding inhibitor/acyl-CoA-binding protein in last instar Manduca sexta midgut. Cell. Tissue Res. **288**, 177-84

20 Chao, H., Zhou, M., McIntosh, A., Schroeder, F. and Kier, A. B. (2003) ACBP and cholesterol differentially alter fatty acyl CoA utilization by microsomal ACAT. J. Lipid Res. **44**, 72-83

21 Helledie, T., Antonius, M., Sorensen, R. V., Hertzel, A. V., Bernlohr, D. A., Kolvraa, S., Kristiansen, K. and Mandrup, S. (2000) Lipid-binding proteins modulate ligand-dependent trans-activation by peroxisome proliferator-activated receptors and localize to the nucleus as well as the cytoplasm. J. Lipid Res. **41**, 1740-51

22 Hansen, J. S., Villadsen, J. K., Gaster, M., Faergeman, N. J. and Knudsen, J. (2006) Micro method for determination of nonesterified fatty acid in whole blood obtained by fingertip puncture. Anal. Biochem. **355**, 29-38

23 Wadum, M. C., Villadsen, J. K., Feddersen, S., Moller, R. S., Neergaard, T. B., Kragelund, B. B., Hojrup, P., Faergeman, N. J. and Knudsen, J. (2002) Fluorescently

labelled bovine acyl-CoA-binding protein acting as an acyl-CoA sensor: interaction with CoA and acyl-CoA esters and its use in measuring free acyl-CoA esters and non-esterified fatty acids. Biochem. J. **365**, 165-72

24 Fisher, C. L. and Pei, G. K. (1997) Modification of a PCR-based site-directed mutagenesis method. Biotechniques **23**, 570-1, 574

25 Faergeman, N. J., Sigurskjold, B. W., Kragelund, B. B., Andersen, K. V. and Knudsen, J. (1996) Thermodynamics of ligand binding to acyl-coenzyme A binding protein studied by titration calorimetry. Biochemistry **35**, 14118-26

26 Schmid, E., Franke, W. W., Grund, C., Schiller, D. L., Kolb, H. and Paweletz, N. (1983) An epithelial cell line with elongated myoid morphology derived from bovine mammary gland. Expression of cytokeratins and desmosomal plaque proteins in unusual arrays. Exp. Cell Res. **146**, 309-28

27 Rudland, P. S., Hallowes, R. C., Durbin, H. and Lewis, D. (1977) Mitogenic activity of pituitary hormones on cell cultures of normal and carcinogen-induced tumor epithelium from rat mammary glands. J. Cell. Biol. **73**, 561-77

28 Schmid, E., Schiller, D. L., Grund, C., Stadler, J. and Franke, W. W. (1983) Tissue type-specific expression of intermediate filament proteins in a cultured epithelial cell line from bovine mammary gland. J. Cell. Biol. **96**, 37-50

29 Li, Q., Lau, A., Morris, T. J., Guo, L., Fordyce, C. B. and Stanley, E. F. (2004) A syntaxin 1, Galpha(o), and N-type calcium channel complex at a presynaptic nerve terminal: analysis by quantitative immunocolocalization. J. Neurosci. **24**, 4070-81

30 Parasassi, T., De Stasio, G., Ravagnan, G., Rusch, R. M. and Gratton, E. (1991) Quantitation of lipid phases in phospholipid vesicles by the generalized polarization of Laurdan fluorescence. Biophys J **60**, 179-89

31 Tricerri, M. A., Toledo, J. D., Sanchez, S. A., Hazlett, T. L., Gratton, E., Jonas, A. and Garda, H. A. (2005) Visualization and analysis of apolipoprotein A-I interaction with binary phospholipid bilayers. J. Lipid Res. **46**, 669-78

32 Kampf, J. P. and Kleinfeld, A. M. (2004) Fatty acid transport in adipocytes monitored by imaging intracellular free fatty acid levels. J. Biol. Chem. **279**, 35775-80

33 Richieri, G. V., Anel, A. and Kleinfeld, A. M. (1993) Interactions of long-chain fatty acids and albumin: determination of free fatty acid levels using the fluorescent probe ADIFAB. Biochemistry **32**, 7574-80

34 Patterson, G. H. and Piston, D. W. (2000) Photobleaching in two-photon excitation microscopy. Biophys. J. **78**, 2159-62

35 Hao, M., Mukherjee, S. and Maxfield, F. R. (2001) Cholesterol depletion induces large scale domain segregation in living cell membranes. Proc. Natl. Acad. Sci. U. S. A. **98**, 13072-7

36 Gerdes, H. H. and Kaether, C. (1996) Green fluorescent protein: applications in cell biology. FEBS Lett **389**, 44-7

37 Faergeman, N. J., Black, P. N., Zhao, X. D., Knudsen, J. and DiRusso, C. C. (2001) The Acyl-CoA synthetases encoded within FAA1 and FAA4 in Saccharomyces cerevisiae function as components of the fatty acid transport system linking import, activation, and intracellular Utilization. J. Biol. Chem. **276**, 37051-9

38 Rolf, B., Oudenampsen-Kruger, E., Borchers, T., Faergeman, N. J., Knudsen, J., Lezius, A. and Spener, F. (1995) Analysis of the ligand binding properties of recombinant bovine liver-type fatty acid binding protein. Biochim. Biophys. Acta **1259**, 245-53

39 Fulceri, R., Knudsen, J., Giunti, R., Volpe, P., Nori, A. and Benedetti, A. (1997) Fatty acyl-CoA-acyl-CoA-binding protein complexes activate the Ca2+ release channel of skeletal muscle sarcoplasmic reticulum. Biochem. J. **325 (Pt 2)**, 423-8

40 Krisans, S. K., Mortensen, R. M. and Lazarow, P. B. (1980) Acyl-CoA synthetase in rat liver peroxisomes. Computer-assisted analysis of cell fractionation experiments. J. Biol. Chem. **255**, 9599-607

41 Drecktrah, D., Chambers, K., Racoosin, E. L., Cluett, E. B., Gucwa, A., Jackson, B. and Brown, W. J. (2003) Inhibition of a Golgi complex lysophospholipid acyltransferase induces membrane tubule formation and retrograde trafficking. Mol. Biol. Cell **14**, 3459-69

42 Fernandez-Hernando, C., Fukata, M., Bernatchez, P. N., Fukata, Y., Lin, M. I., Bredt, D. S. and Sessa, W. C. (2006) Identification of Golgi-localized acyl transferases that palmitoylate and regulate endothelial nitric oxide synthase. J. Cell. Biol. **174**, 369-77

43 Glick, B. S. and Rothman, J. E. (1987) Possible role for fatty acyl-coenzyme A in intracellular protein transport. Nature **326**, 309-12

44 Ostermann, J., Orci, L., Tani, K., Amherdt, M., Ravazzola, M., Elazar, Z. and Rothman, J. E. (1993) Stepwise assembly of functionally active transport vesicles. Cell **75**, 1015-25

45 Pfanner, N., Glick, B. S., Arden, S. R. and Rothman, J. E. (1990) Fatty acylation promotes fusion of transport vesicles with Golgi cisternae. J. Cell. Biol. **110**, 955-61

46 Pfanner, N., Orci, L., Glick, B. S., Amherdt, M., Arden, S. R., Malhotra, V. and Rothman, J. E. (1989) Fatty acyl-coenzyme A is required for budding of transport vesicles from Golgi cisternae. Cell **59**, 95-102

47 Vincent, M. J., Martin, A. S. and Compans, R. W. (1998) Function of the KKXX motif in endoplasmic reticulum retrieval of a transmembrane protein depends on the length and structure of the cytoplasmic domain. J. Biol. Chem. **273**, 950-6

48 Burton, M., Rose, T. M., Faergeman, N. J. and Knudsen, J. (2005) Evolution of the acyl-CoA binding protein (ACBP). Biochem. J. **392**, 299-307

49 Chao, H., Martin, G. G., Russell, W. K., Waghela, S. D., Russell, D. H., Schroeder, F. and Kier, A. B. (2002) Membrane charge and curvature determine interaction with acyl-CoA binding protein (ACBP) and fatty acyl-CoA targeting. Biochemistry **41**, 10540-53

50 Taskinen, J., van Aalten, D. M. F., Knudsen, J. and Wierenga, R. K. (2006) High resolution crystal structures of unliganded and liganded human liver ACBP reveal a new mode of binding for the acyl-CoA ligand. Proteins, In press

FIGURE LEGENDS

Figure 1 GFP-ACBP and GFP localization *in vivo* in HeLa cells

HeLa cells were stably transfected with GFP-ACBP or the empty pEGFP-C1 vector alone, respectively. GFP fluorescence was excited at 488 nm with a 30-mW Argon/2 laser and images were collected using a primary HFT 488 dichroic beam splitter and a 505 nm long pass filter. The nucleus of GFP-transfected cells were identified by incubating cells for 60 minutes with 16 μM of DAPI dissolved in C-HEPES buffer. DAPI was excited at 800 nm using two-photon excitation, which was reflected by a primary HFT KP 650 dichroic mirror, fluorescence filtered with a secondary NFT 490 dichroic mirror and emission recorded with a 435-485 nm band pass filter.

Figure 2 ACBP localization with ER in BMGE cells is function dependent

Localization of microinjected FACI-50 (A, top left panel) or Y28F/K32A-FACI-50 (B, top left panel) and ER tracker glibenclamide-BODIPY TR (A and B, top midle panel), in BMGE cells. Merged images are presented in top right panels. Lower left panels show scatter plot of FACI-50 (A) and Y28F/K32A-FACI-50 (B) pixel staining intensities against ER tracker glibenclamide-BODIPY TR pixel staining intensities. Lower centre and right panels, show individual fluorescence intensities of FACI-50 (A, lower middle panel), Y28F/K32A-FACI-50 (B, lower middle panel) or glibenclamide-BODIPY TR (lower right panels) plotted against their respective PDM values of both recording channels.

Figure 3 ACBP localizes to Golgi in a ligand-binding dependent manner

Localization of microinjected FACI-50 (A, top left panel), Y28F/K32A-FACI-50 (B, top left panel) and Golgi marker BODIPY TR C_5-ceramide (A and B, top middle panel) in BMGE cells. Merged images are presented in top right panels. Lower left panels show scatter plot of FACI-50 (A) and Y28F/K32A-FACI-50 (B) pixel staining intensities against Golgi marker BODIPY TR C_5-ceramide pixel staining intensities. Lower centre and right panels, show individual fluorescence intensities of FACI-50 (A, lower middle panel), Y28F/K32A-FACI-50 (B, lower middle panel) or Golgi marker BODIPY TR C_5-ceramide (lower right panels) plotted against their respective PDM values of both recording channels.

Figure 4 FAFBSA and OA/BSA challenging of FACI-50 injected BMGE cells

A) FACI-50 (upper panels) and Golgi marker BODIPY TR C_5-ceramide (lower panels) localization in BMGE cells incubated successively for 10 min in C-HEPES buffer (left), C-HEPES buffer containing FAFBSA (600 μM) and in and C-HEPES buffer containing OA/BSA (molar ratio 0.6/2.64 mM, to give a calculated free OA concentration of 150 nM [32, 33]). B) Shows the intensity correlation coefficients (ICQ) for FACI-50 fluorescence correlation with Golgi staining under the conditions described above. Results are means ± S.D. (n = 5). Asterisk indicates statistical differences ($p < 0.001$) between ICQ values obtained for cells in C-HEPES/FAFBSA buffer relative to the same cells incubated in C-HEPES buffer and C-HEPES/OA/BSA buffer, respectively.

Figure 5 Normalized FACI-50 spectra and GP measurements in BMGE cells

A) Normalized emission spectra of 1 μM FACI-50 in the absence (□) or presence of saturating amounts of CoA (△) or oleyl-CoA (◇). B) Histogram of whole cell GP measurements in FACI-50 injected BMGE cells.

Figure 6 Fluorescence recovery after photobleaching of FACI-50 in Golgi

An image was acquired FACI-50 injected BMGE cells in C-HEPES buffer and cells incubated for 20 minutes with OA/BSA buffer (molar ratio 0.6/2.64 mM), respectively. A region of interest (ROI) of the Golgi was photobleached for a very brief period by two-photon laser excitation (45% output) at 800 nm. Images were taken at different time points after photobleaching to monitor the fluorescence recovery. After background correction, a ratio of fluorescence intensities in a photobleached region vs. the whole cell was calculated for each time point. This ratio was divided by the corresponding ratio obtained from the pre-bleaching image and presented as the percentage recovered. Each data point, derived from an average of 5 experiments, was fitted to the equation $y = y_0 + a\,(1\text{-}e^{-kt})$ by SIGMAPLOT scientific graphing software, where k is the rate constant. Values are means ± S.D. (n = 5). Half recovery times ($t_{½}$) were calculated according to $t_{½} = \ln(2)/k$.

Biochemical Journal Immediate Publication. Published on 22 Oct 2007 as manuscript BJ20070559

FIGURES

Figure 1

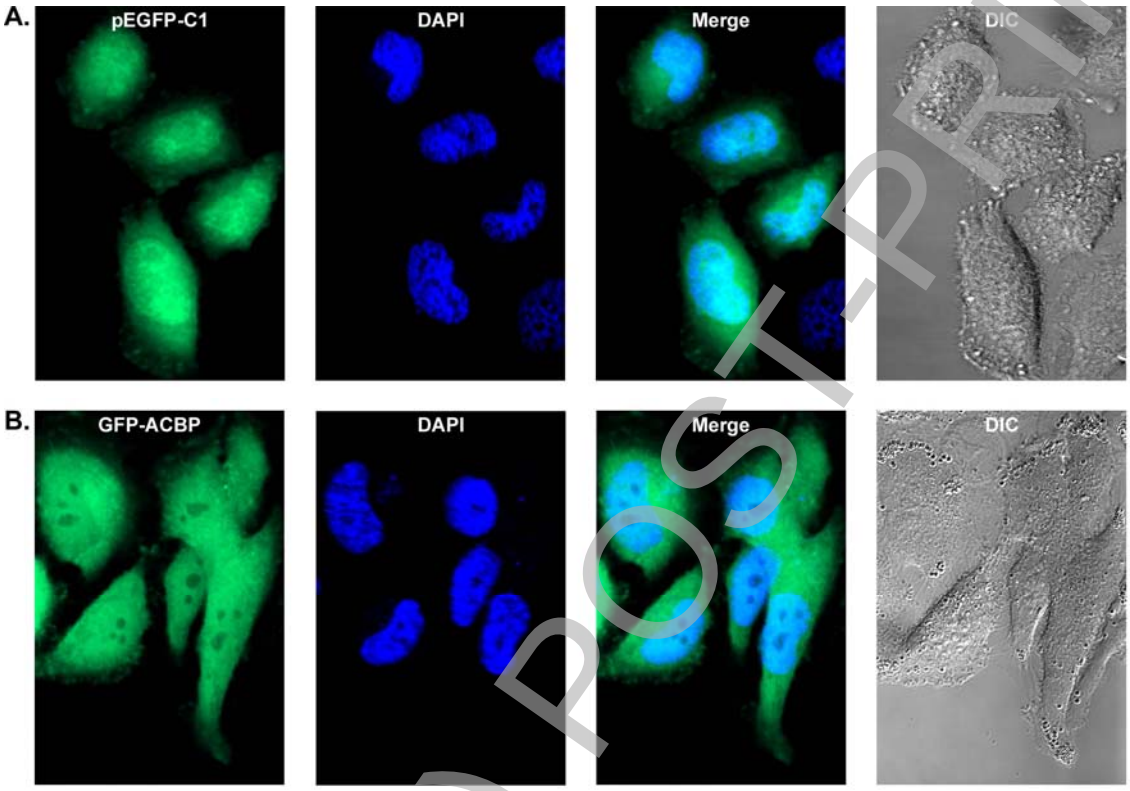

Figure 2

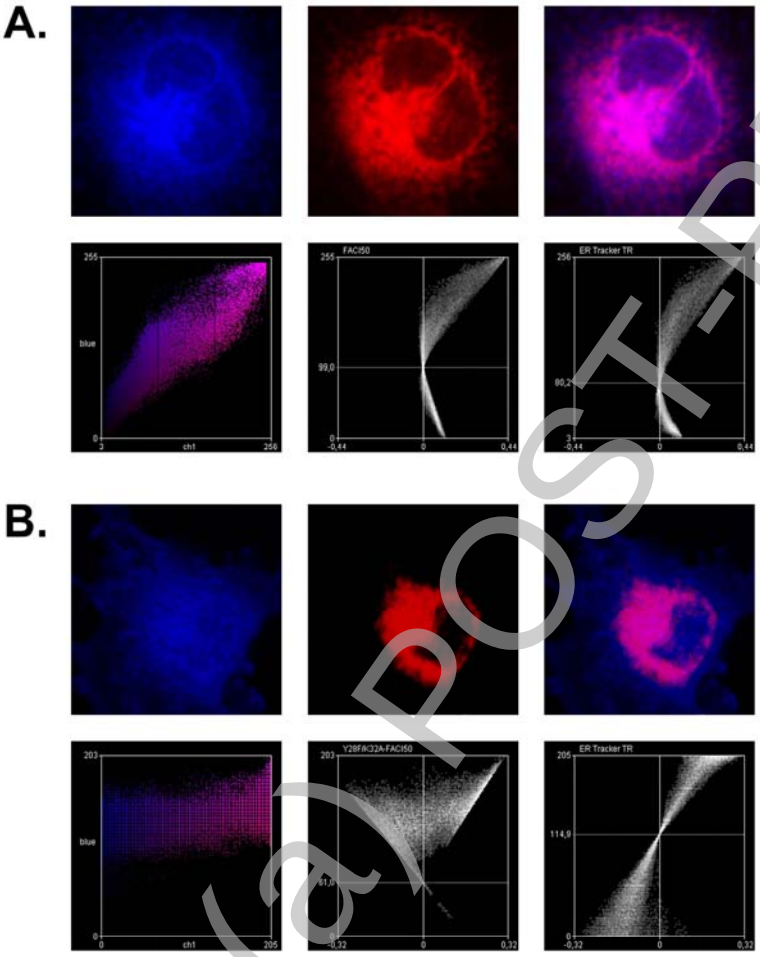

Figure 3

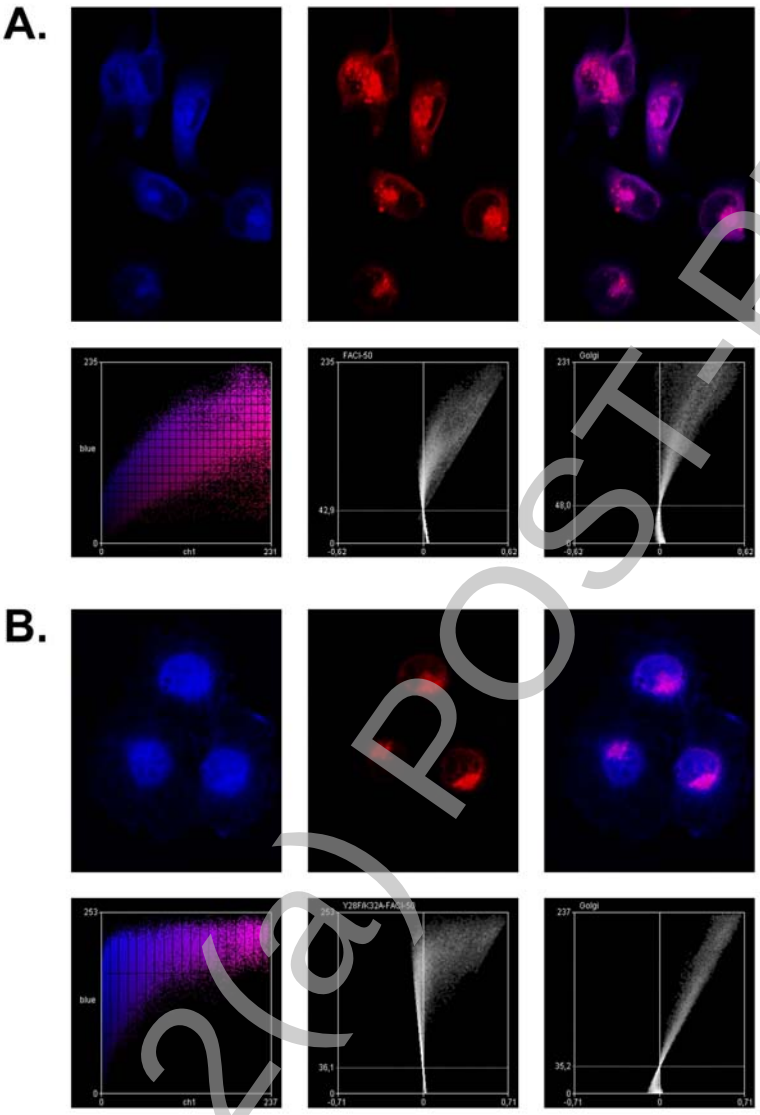

Figure 4

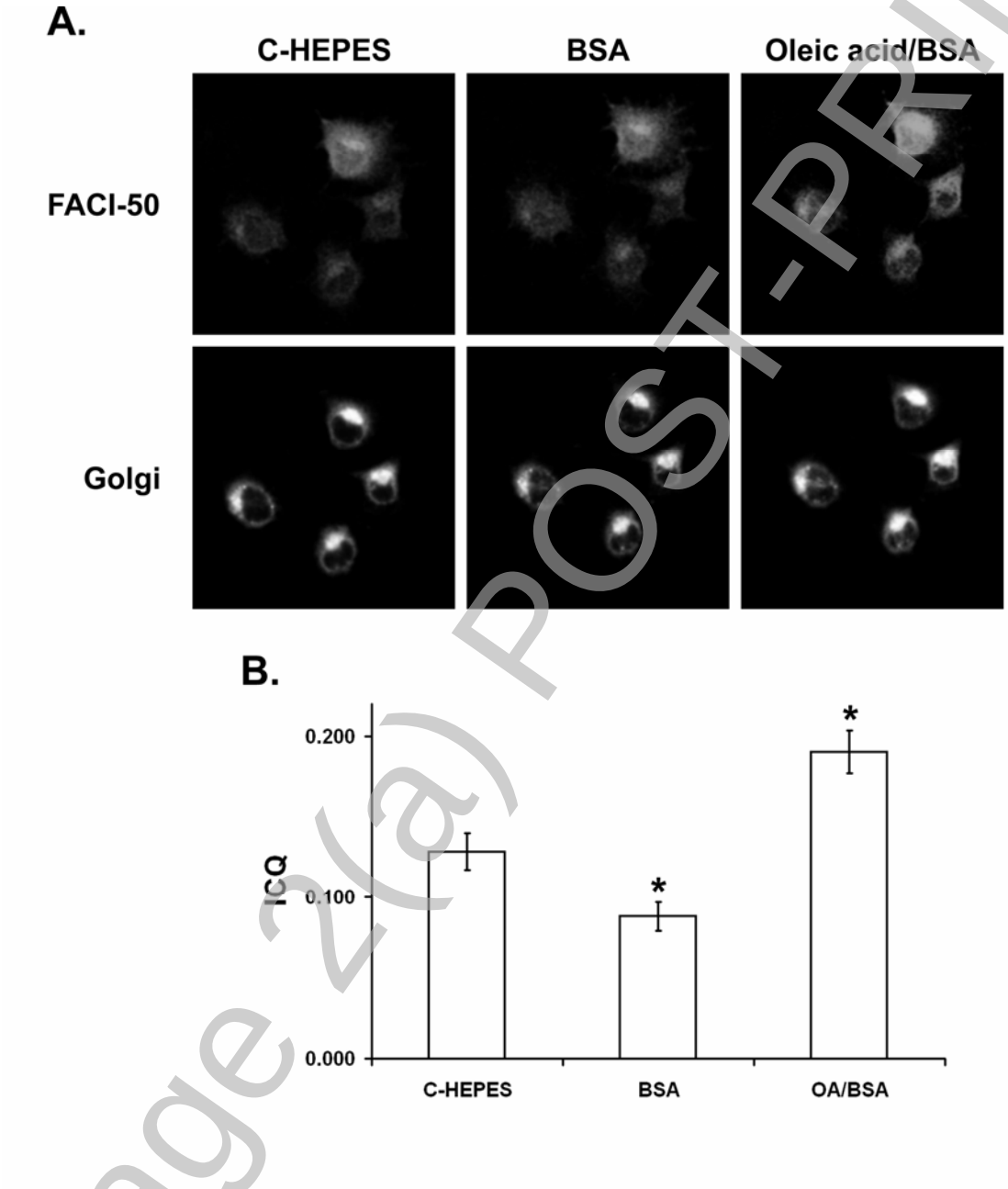

Figure 5

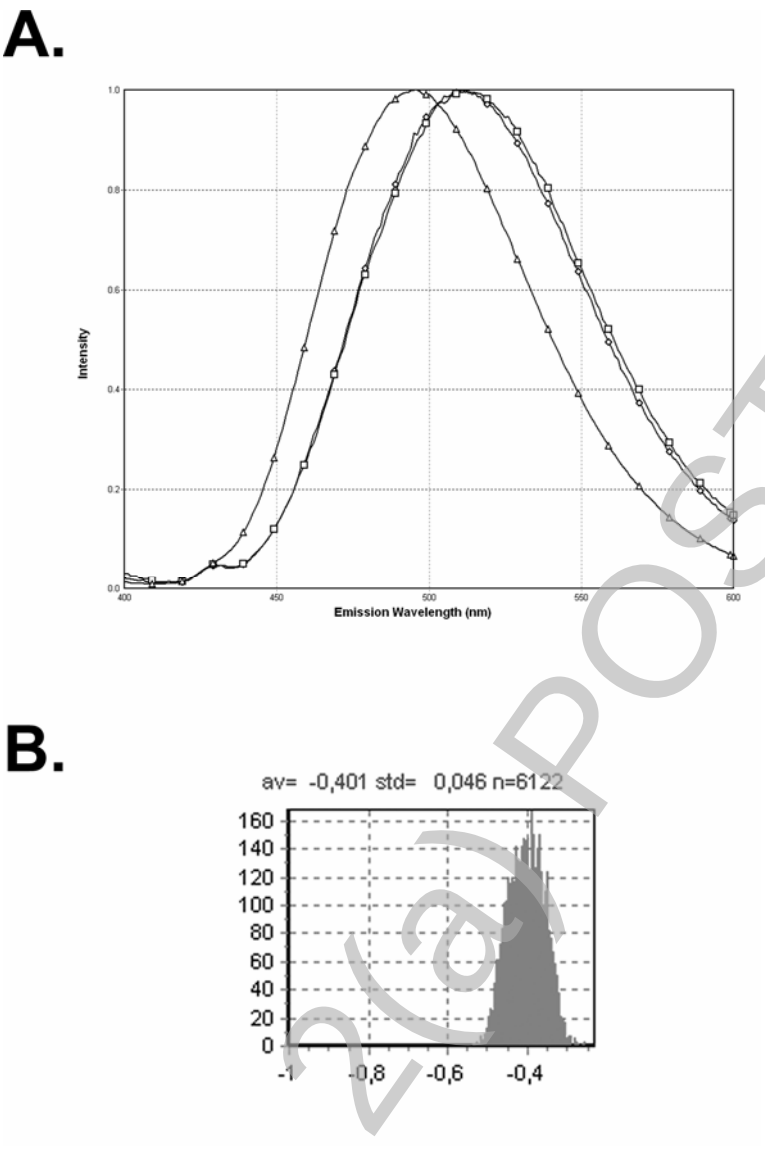

Figure 6